Published in final edited form as:
Eur J Med Chem. 2013 October ; 68: 473–481. doi:10.1016/j.ejmech.2013.07.018.

Selective cytotoxicity, inhibition of cell cycle progression, and induction of apoptosis in human breast cancer cells by sesquiterpenoids from *Inula lineariifolia* Turcz.

Jiang-Jiang Qin[#a,c], **Hui-Zi Jin**[#a], **Ying Huang**[a], **Shou-De Zhang**[a], **Lei Shan**[b], **Sukesh Voruganti**[c], **Subhasree Nag**[c], **Wei Wang**[c], **Wei-Dong Zhang**[a,b,*], and **Ruiwen Zhang**[c,**]

[a]School of Pharmacy, Shanghai Jiao Tong University, Shanghai 200240, PR China

[b]Department of Phytochemistry, Second Military Medical University, Shanghai 200433, PR China

[c]Department of Pharmaceutical Sciences, School of Pharmacy, Texas Tech University Health Sciences Center, Amarillo, TX 79106, USA

[#] These authors contributed equally to this work.

Abstract

Four new sesquiterpenoid dimers (lineariifolianoids E–H, **1**–**4**), five new sesquiterpenoids (**5**–**9**), and seven known sesquiterpenoids (**10**–**16**) were isolated from the aerial parts of *Inula lineariifolia* Turcz. Their structures were determined by spectroscopic data analysis and X-ray diffraction studies. The compounds were then evaluated for their *in vitro* cytotoxicity against two human breast cancer cell lines (MCF-7 and MDA-MB-231) and one normal breast cell line (MCF-10A). Lineariifolianoid E (**1**) showed IC_{50} values of 1.56 μM and 2.75 μM against MCF-7 and MDA-MB-231, respectively. However, lineariifolianoid E demonstrated low toxicity to MCF-10A cells, which indicated a selective cytotoxicity for tumor cells. Further studies also presented that lineariifolianoid E had significant, dose-dependent effects on cell cycle progression and apoptosis in breast cancer cells.

Keywords

Inula lineariifolia Turcz.; Sesquiterpenoid; Cytotoxicity; Breast cancer; Cell cycle arrest; Apoptosis

[*]**Correspondence:** Dr. Wei-Dong Zhang, School of Pharmacy, Shanghai Jiao Tong University, Dongchuan Rd 800, Shanghai 200240, China. Tel: +86-21-34205989; Fax: +86-21-34205989; wdzhangy@hotmail.com.. [**]**Correspondence:** Dr. Ruiwen Zhang, Department of Pharmaceutical Sciences, Texas Tech University Health Sciences Center, 1300 S. Coulter Street, Amarillo, TX 79106, USA; Tel: 806-356-4750 ext 230; Fax: 806-356-4034; ruiwen.zhang@ttuhsc.edu.

1. Introduction

Inula, a medically important genus in the family Asteraceae, encompasses about 100 species and is widely distributed throughout the world, especially in Mediterranean countries of Europe, Africa, and Asia [1]. Some of species from this genus have long been used as folk medicine for anti-inflammatory and anticancer activities [2]. The extracts of *Inula* plants also display high diverse biological activities, such as anti-inflammatory [3–10], anti-tumor [11–13], antimicrobial [14–16] and hepatoprotective effects [17–18]. However, the main components in these plants have been reported as sesquiterpenoids [2, 4–16, 19–20]. Sesquiterpenoids are well known for the high diversity in their structures and biological activities [21]. The α-methylene-γ-lactone ring, a common functional group in guaiane sesquiterpenoids, as well as other chemical properties, lead to their promising anticancer effects, and also make them reach cancer clinical trials, such as artemisinin, thapsigargin, parthenolide and many of their synthetic derivatives [21–22].

Inula linearіifolia Turcz. is widely distributed in China and its aerial parts are used in the traditional Chinese medicine “JinFeiCao” [1, 6, 19]. Previously, fourteen sesquiterpenoids and four sesquiterpenoid dimers with anti-inflammatory effects have been reported from the aerial parts of *I. linearіifolia* [6, 19]. This study was designed to investigate the anticancer components in this medicinal plant and resulted in the isolation and identification of four new sesquiterpenoid dimers (linearіifolianoids E–H, **1**–**4**), five new sesquiterpenoids (**5**à**9**), and seven known sesquiterpenoids (**10**–**16**) (Fig. 1). The *in vitro* cytotoxicity of the compounds were evaluated in two human breast cancer cell lines (MCF-7 and MDA-MB-231) and one normal breast cell line (MCF-10A). The most effective compound, linearіifolianoid E (**1**) showed selective cytotoxicity against breast cancer cells. Further investigation indicated that linearіifolianoid E induced cell cycle arrest and apoptosis in the breast cancer cells. The present study may provide a basis for the future development of this class of sesquiterpenoid dimers as novel anti-breast cancer agents.

2. Results and discussion

2.1 Isolation and structure elucidation

The CH_2Cl_2 soluble part of the EtOH extract from the aerial parts of *I. linearіifolia* was fractionated by silica gel column chromatography, followed by Sephadex LH-20 and preparative HPLC to afford four new sesquiterpenoid dimers (linearіifolianoids E–H, **1**–**4**), five new sesquiterpenoids (**5**–**9**), and seven known sesquiterpenoids: deacetylinuchinenolide B (**10**) [23–24], inuchinenolide B (**11**) [23], britanlin G (**12**) [23, 25], 2α-acetoxy-4α,6α-dihydroxy-1β,5αH-guai-9(10),11(13)-dien-12,8α-olide (**13**) [9], bigelovin (**14**) [9], 3β-hydroxy-11α,13-dihydroalantolactone (**15**) [26], and deacetylovatifolin (**16**) [27] (Fig. 1).

Linearіifolianoid E (**1**) was obtained as white amorphous powder and shown to have the molecular formula $C_{32}H_{42}O_8$ from HRESIMS (*m/z* 577.2774 for $[M+Na]^+$, calcd *m/z* 577.2772), indicating 12 degrees of unsaturation. The IR absorptions showed the presence of hydroxyl (3424 cm^{-1}), carbonyl (1767 and 1722 cm^{-1}), and olefinic groups (1631 cm^{-1}). The ^{13}C, DEPT, and HSQC NMR spectra of **1** (Table 1) exhibited 32 carbon signals, which revealed the presence of five methyls, seven methylenes, eleven methines, and nine

quaternary carbons including three carbonyl groups. The ^{1}H and ^{13}C NMR spectra also suggested the presence of an acetoxy group (δ_H 2.01, δ_C 170.7 and 21.1), and its position was determined by HMBC experiment (Fig. 2). Detailed analysis of 1D and 2D NMR data of the remaining 30 carbon signals revealed that they belonged to two different sesquiterpenoid moieties, A_1 and B_1. Upon comparison with the spectral data of other sesquiterpenoid dimers isolated from genus *Inula* [5, 11, 19], an identical guaianolide skeleton moiety (moiety A_1) (Fig. 2) with a characteristic α-methylene lactone functionality can be authenticated by olefinic carbons C-11′ (δ_C 139.7) and C-13′ (δ_C 118.9), and exocyclic olefinic protons H-13′a (δ_H 6.25) and H-13′b (δ_H 5.60). ^{1}H-^{1}H COSY and HMBC correlations (Fig. 2) also established the other moiety (moiety B_1), similar to 2-*O*-acetyl-4-epipulchellin [28], which was previously isolated from this plant [6]. Compared with 2-*O*-acetyl-4-epipulchellin, the spectroscopic data of moiety B_1 mainly differed in the chemical shifts of C-11 and C-13, suggesting that the two moieties were connected through these units. The key HMBC correlations from H-2′ to C-11 and C-13; H-3′ to C-7 and C-13, and H-13 to C-2′ and C-5′ indicated the presence of a bridged ring system, a norbornene moiety (Fig. 2) [5, 11, 19].

The stereochemistry of **1** was determined on the basis of NOESY experiment (Fig. 3) and the comparison of compound **1**'s NMR data with those reported. The strong NOESY correlations of H-2′/H-3′, H-8′ and H_3-14′; H-3′/H-7; H-8′/H_3-14′ were observed in moiety A_1, indicating that H-2′, H-3′, H-8′, H_3-14′, H-7 and H-8 adopted the same orientation. Because compound **1** has the same guaianolide skeleton moiety as Japonicone A and Lineariifolianoid A, whose absolute configurations have been established [11, 19], it could be speculated that H-2′, H-3′, H-8′, H_3-14′, H-7 and H-8 were α-orientated. In addition, the correlations of H-4/H-7; H-1/H-4 and H_3-14 also suggested that H-1, H-4, H-7, and H_3-14 were α-orientated. Further analysis of NOESY spectrum also showed the correlations between H-2/H-10, H-2/H_3-15, H-8/H-10, and H-8/H_3-15, which indicated that they were cofacial and β-orientated.

Lineariifolianoids F (**2**) and G (**3**) with molecular formula of $C_{34}H_{42}O_9$ and $C_{32}H_{40}O_8$ as established from their HRESIMS at *m/z* 617.2730 $[M+Na]^+$ and 575.2640 $[M+Na]^+$, respectively, showed similar NMR spectroscopic data, except for an additional acetoxy group (δ_H 2.09, δ_C 170.6 and 21.2) attached at C-2′ in **2**. The ^{1}H and ^{13}C data of **2** and **3** (Table 1) indicated that they were also sesquiterpenoid dimers and both had two guaianolide skeleton moieties. Compared with the spectral data of known sesquiterpenoids isolated from this plant [6], the other moiety of **2** and **3** was determined as gaillardin [23], which was also confirmed by the detailed analysis of 2D NMR data. The presence of a hydroxyl group at δ_H 6.18, along with the absence of an acetoxy group suggested that **3** was a deacetylated derivative of **2**. Similar NOEs of the guaianolide moiety to those observed in **1** suggested the same stereochemistry. The relative configuration of gaillardin moiety was mainly deduced from NOESY correlations of H-7/H-5 and H-1/H-2, H-8 and H_3-15.

Lineariifolianoid H (**4**) was obtained as colorless gum and shown to have the molecular formula $C_{32}H_{40}O_8$, as determined by its HRESIMS (*m/z* 575.2628 for $[M+Na]^+$, calcd *m/z* 575.2615), indicating 13 degrees of unsaturation. The IR spectrum showed the presence of hydroxyl (3429 cm^{-1}), carbonyl (1747 cm^{-1}), and olefinic groups (1634 cm^{-1}). The ^{1}H

and ^{13}C NMR spectroscopic data of **4** (Table 1) were very similar to those reported for inulanolide B [4], except that a methyl (δ_C 20.1, H_3-14) in inulanolide B was replaced by an oxygenated methylene (δ_C 60.6, C-14) in **4**. Similar relative configuration with inulanolide B was deduced by the analysis of NOESY data; the key NOESY correlations included H-5/H-7, H-6/H_3-15, H-7/H-8, H-7/H-3′, H-2′/H-3′, H-2′/H_3-14′, and H-8′/H_3-14′. Furthermore, a single crystal X-ray crystallographic measurement of **16** (Fig. 4) was also supported the relative configuration of the deacetylovatifolin moiety in **4**.

Compounds **5** and **6** were assigned the molecular formula $C_{15}H_{20}O_4$ and $C_{15}H_{20}O_5$ from their HRESIMS at *m/z* 287.1255 and 303.1207 $[M+Na]^+$, respectively. The NMR data of **5** (Table 2) were very similar to those of 2α-acetoxy-4α-hydroxy-1β-guai-11(13),10(14)-dien-12,8α-olide [6], except for the absence of an acetoxy group. In the NOESY spectrum, correlations between H-1/H-2, H-1/H-8, H-1/H_3-15, and H-5/H-7 were observed. These observations together with a 42 Da mass minus indicated that **5** was a deacetylated derivative of the above compound, and named as 2α,4α-dihydroxy-1β-guai-11(13),10(14)-dien-12,8α-olide. Similarly, **6** was elucidated as a deacetylated derivative of 5α,6α-epoxy-2α-acetoxy-4α-hydroxy-1β,7α-guaia-11(13)-en-12, 8α-olide [6]. The NOESY correlations between H-1/H-2, H-1/H-10, H-2/H-10, H-2/H_3-15, H-6/H-8, H-6/H_3-15, and H-8/H-10 were observed. Compound **6** was named as 5α,6α-epoxy-2α,4α-dihydroxy-1β-guai-11(13)-en-12,8α-olide.

Compound **7** showed a molecular formula $C_{17}H_{22}O_6$ by the positive HRESIMS ion at *m/z* 345.1308 $[M+Na]^+$. The ^{1}H and ^{13}C NMR spectra of **7** (Table 2) were very similar with those of inuchinenolide B (**11**) except that an oxygenated methine (δ_C 71.3, C-6) in **7** replaced the methylene (δ_C 26.3, C-6) in inuchinenolide B [23]. These observations together with a 16 Da mass surplus indicated that **7** was a hydroxylated derivative of inuchinenolide B. Detailed analysis of ^{1}H-^{1}H COSY and HMBC spectra further confirmed the structure of **7**. The important NOESY correlations of H_3-15/H-6 and H-2 indicated that the hydroxyl at C-6 was α-orientated. Compound **7** was then elucidated as 6α-hydroxyinuchinenolide B.

Compound **8** was obtained as colorless orthorhombic crystal, and assigned the molecular formula $C_{17}H_{24}O_5$ from HRESIMS (*m/z* 331.1521 for $[M+Na]^+$, calcd *m/z* 331.1516). The NMR data of **8** (Table 2) resembled those of the reported 2-*O*-acetyl-4-epipulchellin [28], suggesting that they may have the same structure, which was also consistent with the 2D NMR data. The relative configuration of **8** was confirmed by single-crystal X-ray diffraction (Fig. 4), which was consistent with the NOESY correlations of H-4/H-1 and H-7; H-8/H-1, H-7 and H-10; H-2/H_3-14 and H_3-15; and H_3-14/H_3-15. Hence, compound **8** was identified as 2α-acetoxy-4β-hydroxy-1αH,10αH-pseudoguai-11(13)-en-12,8β-olide.

Compound **9** had the molecular formula $C_{15}H_{22}O_5$, as established from its HRESIMS at *m/z* 305.1370 $[M+Na]^+$. The ^{1}H and ^{13}C NMR data of **9** (Table 2) resembled those of the reported sundiversifolide [29], except for an additional acetoxyl group (δ_H 1.95, δ_C 171.8 and 21.2); its position was determined by the HMBC correlation of H-6 (δ_H 5.14) to the carbonyl (δ_C 171.8). The acetoxyl group attached to C-6 was assigned as β-orientated based on the coupling constant (0 Hz) between H-6 and H-7 [6, 23]. In the NOESY spectrum,

correlations between H-6/H-7, H-7/H-8, H-7/H-11, and H-8/H-10 were observed. Therefore, the structure of **9** was identified as 6β-acetoxysundiversifolide.

2.2 Biological activity of sesquiterpenoids and sesquiterpenoid dimers

2.2.1 Initial screening for growth inhibition in human breast cancer cells and normal breast cells—Sixteen compounds (**1–16**) were tested for their *in vitro* anticancer activity using MTT assay. Doxorubicin and paclitaxel were selected as the positive controls in this study. Two human breast cancer cell lines (MCF-7 and MDA-MB-231) and one normal breast cell line (MCF-10A) were cultured with test compounds (**1–16**) at concentration ranging from 1 μM to 50 μM for 72 h, then cell viability was determined. As illustrated in Table 3, most of the compounds showed impressive activity against MCF-7 and MDA-MB-231 cells. However, the normal breast cell line MCF-10A was less sensitive to the inhibitory effects of these compounds than the breast cancer cell lines, indicating the selective cytotoxicity of the compounds for cancer cells. The IC_{50} values also showed that the sesquiterpenoid dimers (**1–4**) exhibited greater inhibitory effects than monomers (**5–16**), which may be attributed to the enhanced cellular penetration after dimerization of these monomers. Many reports have demonstrated the important role of α-methylene-γ-lactone moiety for the biological activity of sesquiterpenoids [21, 30–32]. This study also provided indirect evidences linking their cytotoxicity to this functionality. The sesquiterpenoids without α-methylene-γ-lactone (**9** and **15**) did not exhibit any noticeable activity against cancer cells even at concentration of 50 μM. Additionally, some sesquiterpenoids with α-methylene-γ-lactone (compounds **6**, **7**, and **10**) also did not show visible activity, which could be explained by the decreased lipophilicity due to the presence of an epoxide group in **6**, or the additional hydroxyl group in **7** and **10** as compared with **11** [7, 9]. Moreover, it has also been reported that an α,β-unsaturated cyclopentenone might cause greater cytotoxic effects than the α-methylene-γ-lactone group [21, 33–34]. In this study, our data showed that compound **14** with both α,β-unsaturated cyclopentenone and α-methylene-γ-lactone groups exhibited similar cytotoxicity as the sesquiterpenoid dimer **1**, which further reinforced the importance of the two functionalities.

2.2.2 Examination of the effects of lineariifolianoid E (1) on the cell cycle—Although the MTT assay provided a general view of the cytotoxicity of these compounds, the mechanisms of action are still not clear. As a hallmark of tumor cells, cell cycle dysregulation contributes to the aberrant cell proliferation and development of cancer [35–36]. Therefore, targeting cell cycle progression presents an effective mothod for novel anticancer drug discovery. To determine whether the inhibitory effects of these sesquiterpenoids on cancer cell growth were correlated with cell cycle arrest, we further investigated the effects of lineariifolianoid E (**1**) on cell cycle progression. As shown in Fig. 5A and B, lineariifolianoid E induced dose-dependent cell cycle arrest in the G2/M phase in MCF-7 cells, but it caused a dose-dependent cell cycle arrest in both S and G2/M phase in MDA-MB-231 cells. At the 2.5 μM concentration, a majority of the MCF-7 cells were arrested in the G2/M phase. However, in MDA-MB-231 cells, lineariifolianoid E at the same concentration led to a significant increase in the number of cells in both S and G2/M phases.

2.2.3 Induction of apoptosis in human cancer cells—Most of currently used anticancer drugs can induce cancer cell apoptosis, however, targeting apoptosis is still considered as one the major strategies for developing anticancer therapeutic agents [37–38]. In the present study, we also examined the effects of linearіifolianoid E (**1**) on cell apoptosis. As illustrated in Fig. 5C, linearіifolianoid E induced apotosis in a dose-dependent manner in both breast cancer cell lines. In the MCF-7 and MDA-MB-231 cells, a 5 μM linearіifolianoid E increased the apoptotic index 7.6-fold and 14.2-fold, respectively, as compared to that in control cells.

3. Conclusion

The current study reported isolation and structure elucidation of four new sesquiterpenoid dimers (linearіifolianoids E–H, **1–4**), five new sesquiterpenoids (**5–9**), and seven known sesquiterpenoids from the aerial parts of *I. linearіifolia*. Since numerous investigations have demonstrated the anticancer activities of sesquiterpenoids, we then evaluated their inhibitory effects on the growth of breast cancer cells (MCF-7 and MDA-MB-231) and normal breast cells (MCF-10A). The IC_{50} values demonstrated their potent cytotoxicity against cancer cells, but no apparent cytotoxic effects were observed in MCF-10A cells, which indicated a selective cytotoxicity of these sesquiterpenoids toward cancer cells. Previous studies of the structure-activities relationship of sesquiterpenoids have demonstrated the essential roles of α-methylene-γ-lactone and α,β-unsaturated cyclopentenone moieties. This study further provided the evidence to reinforce their roles for the cytotoxicity of sesquiterpenoids. Moreover, we have also revealed that sesquiterpenoid dimers possess more potent anticancer activity than the monomers and that linearіifolianoid E was the most effective candidate among these compounds. In order to further investigate the possible mechanisms that are involved in the inhibitory activity caused by linearіifolianoid E, we examined its effects on cell cycle progression and apoptosis. The results suggested that this sesquiterpenoid dimer induced cell cycle arrest and apoptosis in a dose dependent manner.

In conclusion, the present investigation demonstrated at least four major points: 1) Sesquiterpenoids and sesquiterpenoid dimers are the main anticancer components of the Chinese medicinal herb *I. linearіifolia*; 2) The anticancer activity of the sesquiterpenoids and sesquiterpenoids dimers is dose-, structure-, and cell type-dependent; 3) Sesquiterpenoids dimers could have better drug-like properties than their monomers; 4) Induction of cell cycle arrest and apoptosis are key mechanisms of action by which linearіifolianoid E exerts its anticancer effects. Further molecular and pharmacological investigations are warranted in order to elucidate the underlying mechanisms of action and to determine the *in vivo* anticancer efficacy of these promising compounds.

4. Material and methods

4.1 General experimental procedures

4.1.1 Instruments—1D and 2D NMR spectra were determined with a Bruker Avance–400 spectrometer in $CDCl_3$ or CD_3OD with TMS as internal standard. Optical rotations were obtained with a JASCO P-2000 polarimeter. IR spectra were recorded on a Bruker FTIR Vector 22 spectrometer using KBr pellets. ESIMS spectra were recorded on an

Agilent–1100–LC/MSD–Trap XCT spectrometer, whereas HRESIMS were performed using a Waters Q–TOF micro mass spectrometer. Column chromatography (CC) was performed on silica gel (100–200, 200–300 mesh, Yantai, China), and Sephadex LH–20 (GE Healthcare Bio-Sciences AB, Sweden). A preparative column (Shimadzu PRC–ODS EV0233) was used for preparative HPLC (Shimadzu LC–6AD).

4.1.2 Chemicals—All chemicals and solvents used were of the highest analytical grade available. Cell culture supplies and media, fetal bovine serum (FBS), horse serum, phosphate-buffered saline (PBS), sodium pyruvate, non-essential amino acids (NEAA), and penicillin-streptomycin were obtained from Invitrogen (Carlsbad, CA).

4.1.3 Plant material—The aerial parts of *Inula linearиifolia* Turcz. were collected in Changfeng County, Anhui Province, PR China, in July 2007, and identified by Dr. Shou-Jin Liu, Anhui University of Traditional Chinese Medicine. A voucher specimen (No. XX20070701) was deposited at School of Pharmacy, Shanghai Jiao Tong University.

4.1.4 Extraction and isolation—The air-dried aerial parts of *I. linearиifolia* (60.0 kg) were powdered and extracted with 95% ethanol three times each for 24 h at room temperature. The solvent was removed in vacuo to afford a crude EtOH extract, which was suspended in H_2O and then partitioned successively with petroleum ether (PE), CH_2Cl_2, EtOAc, and *n*-BuOH, respectively. 150.0 g of the CH_2Cl_2 extract was subjected to silica gel column (10 × 70 cm; 100–200 mesh, 1500 g) eluted with gradient CH_2Cl_2/MeOH (1:0 to 1:1) to give 10 fractions (Fr.1–Fr.10) based on TLC analysis. Fr.2 (33.0 g) was chromatographed (4.5 × 40 cm) on silica gel (200–300 mesh, 660 g) eluted with a gradient of PE/EtOAc (20:1 to 1:1) to afford five subfractions (Fr.2-1–Fr.2-5). Subfraction Fr.2-2 was subjected to preparative HPLC (MeOH/H_2O, 40:60) to give **12** (186.8 mg), **14** (14.5 mg), and **15** (6.0 mg). Fr.4 (15.5 g) was subjected to a silica gel CC (4.5 × 40 cm; 200–300 mesh, 310 g) eluted with gradient PE/EtOAc (5:1 to 1:1) to give eleven subfractions (Fr. 4-1–Fr.4-11). From subfraction Fr.4-4 (1.7 g), compound **7** (22.8 mg) was isolated after CC over Sephadex LH-20 (4.0 × 150 cm; MeOH) followed by preparative HPLC (MeOH/H_2O, 45:55). Fr.4-6 (1.3 g) was chromatographed on silica gel (2.5 × 20 cm; 26 g, 200–300 mesh) eluted with gradient PE/EtOAc (5:1 to 1:1) followed by preparative HPLC (MeOH/H_2O, 40:60) to give **8** (37.0 mg) and **11** (20.4 mg). Compounds **13** (250.0 mg) and **16** (900.0 mg) were crystallized (MeOH) from Fr.4-7 (0.5 g) and Fr.4-8 (1.3 g), respectively. Fr.4-10 (1.2 g) was chromatographed on silica gel (2.5 × 20 cm; 24 g, 200–300 mesh) eluted with gradient CH_2Cl_2/MeOH (1:0 to 1:1) to give five subfractions (Fr.4-10a–Fr.4-10e). Fr.4-10e was subjected to preparative HPLC (MeOH/H_2O, 45:55) to give **5** (17.0 mg) and **6** (4.0 mg), and further eluted with (MeOH/H_2O, 60:40) to yield **1** (36.0 mg) and **4** (24.0 mg). Compounds **2** (18.5 mg), **3** (20.0 mg), and **9** (6.0 mg) were isolated after CC over silica gel (2.5 × 20 cm; 18 g, 200–300 mesh) followed by preparative HPLC (MeOH/H_2O, 55:45) from Fr.4-11 (0.9 g). Fr.6 (0.8 g) was subjected to preparative HPLC (MeOH/H_2O, 40:60) to give 10 (48.0 mg).

*Compound **1***. White amorphous powder; $[\alpha]^{20}_D$ −7.2 (*c* 0.20, MeOH); IR (KBr) ν_{max} 3424, 2933, 1767, 1722, 1631 cm^{-1}; ^1H and ^{13}C NMR data, see Table 1; ESIMS (positive) *m/z*

577 $[M+Na]^+$, HRESIMS (positive) *m/z* 577.2774 $[M+Na]^+$ (calcd for $C_{32}H_{42}O_8Na$, 577.2772).

*Compound **2***. Yellow gum; $[\alpha]^{20}_D$ −15.0(*c* 0.10, MeOH); IR (KBr) ν_{max} 3442, 2969, 1766, 1733, 1636 cm^{-1}; ^1H and ^{13}C NMR data, see Table 1; ESIMS (positive) *m/z* 617 $[M+Na]^+$, HRESIMS (positive) *m/z* 617.2730 $[M+Na]^+$ (calcd for $C_{34}H_{42}O_9Na$, 617.2721).

*Compound **3***. Colorless gum; $[\alpha]^{20}_D$ +10.5 (*c* 0.20, MeOH); IR (KBr) ν_{max} 3424, 2927, 1726, 1631 cm^{-1}; ^1H and ^{13}C NMR data, see Table 1; ESIMS (positive) *m/z* 575 $[M+Na]^+$, HRESIMS (positive) *m/z* 575.2640 $[M+Na]^+$ (calcd for $C_{32}H_{40}O_8Na$, 575.2615).

*Compound **4***. Colorless gum; $[\alpha]^{20}_D$ +0.7 (*c* 0.20, MeOH); IR (KBr) ν_{max} 3429, 2931, 1747, 1634 cm^{-1}; ^1H and ^{13}C NMR data, see Table 1; ESIMS (positive) *m/z* 575 $[M+Na]^+$, HRESIMS (positive) *m/z* 575.2628 $[M+Na]^+$ (calcd for $C_{32}H_{40}O_8Na$, 575.2615).

*Compound **5***. Yellow gum; $[\alpha]^{20}_D$ +21.7(*c* 0.10, MeOH); IR (KBr) ν_{max} 3424, 2925, 1761, 1632 cm^{-1}; ^1H and ^{13}C NMR data, see Table 2; ESIMS (positive) *m/z* 287 $[M+Na]^+$, HRESIMS (positive) *m/z* 287.1255 $[M+Na]^+$ (calcd for $C_{15}H_{20}O_4Na$, 287.1254).

*Compound **6***. Colorless gum; $[\alpha]^{20}_D$ −14.7 (*c* 0.10, MeOH); IR (KBr) ν_{max} 3426, 2926, 1765, 1633 cm^{-1}; ^1H and ^{13}C NMR data, see Table 2; ESIMS (positive) *m/z* 303 $[M+Na]^+$, HRESIMS (positive) *m/z* 303.1207 $[M+Na]^+$ (calcd for $C_{15}H_{20}O_5$ Na, 303.1208).

*Compound **7***. Yellow gum; $[\alpha]^{20}_D$ −9.0 (*c* 0.10, MeOH); IR (KBr) ν_{max} 3469, 2969, 1761, 1709, 1660 cm^{-1}; ^1H and ^{13}C NMR data, see Table 2; ESIMS (positive) *m/z* 345 $[M+Na]^+$, HRESIMS (positive) *m/z* 345.1308 $[M+Na]^+$ (calcd for $C_{17}H_{22}O_6Na$, 345.1309).

*Compound **8***. Colorless orthorhombic crystals (Acetone); mp: 177–179 °C; $[\alpha]^{20}_D$ +40.4 (*c* 0.10, MeOH); IR (KBr) ν_{max} 3453, 2971, 2936, 1730, 1650 cm^{-1}; ^1H and ^{13}C NMR data, see Table 2; ESIMS (positive) *m/z* 331 $[M+Na]^+$, HRESIMS (positive) *m/z* 331.1521 $[M+Na]^+$ (calcd for $C_{17}H_{24}O_5Na$, 331.1516).

*Compound **9***. Colorless gum; $[\alpha]^{20}_D$ +97.3 (*c* 0.10, MeOH); IR (KBr) ν_{max} 3442, 2922, 1738, 1570 cm^{-1}; ^1H and ^{13}C NMR data, see Table 2; ESIMS (positive) *m/z* 305 $[M+Na]^+$, HRESIMS (positive) *m/z* 305.1370 $[M+Na]^+$ (calcd for $C_{15}H_{22}O_5Na$, 305.1359).

*Compound **16***. Colorless orthorhombic crystals (CH_2Cl_2); mp: 164–166 °C [27]; $[\alpha]^{20}_D$ −240.7 (*c* 0.10, MeOH); IR (KBr) ν_{max} 3424, 2954, 1742, 1660 cm^{-1}; ^1H and ^{13}C NMR data, see Table 2; ESIMS (positive) *m/z* 287 $[M+Na]^+$, 265 $[M+H]^+$.

4.2 X-ray crystallography for compounds 8 and 16

Crystallographic data of **8** $C_{17}H_{24}O_5$, *M* = 308.36, orthorhombic, space group P2(1)2(1)2(1), a = 10.0321 (17) Å, α = 90°; b = 12.231 (2) Å, β = 90°; c = 13.457 (2) Å, γ = 90°; *V* = 1651.2 (5) $Å^3$, *Z* = 4, D_{calcd} = 1.240 mg/m^3, crystal size 0.405 × 0.369 × 0.311 mm^3. Mo Kα (λ = 0.71073 Å), *F* (000) = 664, *T* = 296(2) K. The final *R* values were R_1 = 0.0367, and wR_2 = 0.1005, for 11425 observed reflections [I > 2σ (*I*)].

Crystallographic data of **16** $C_{15}H_{20}O_4$, M = 264.31, orthorhombic, space group P2(1)2(1)2(1), a = 9.5551 (8) Å, α = 90°; b = 10.1351 (8) Å, β = 90°; c = 13.9185 (11) Å, γ = 90°; V = 1347.89 (19) $Å^3$, Z = 4, D_{calcd} = 1.302 mg/m^3, crystal size 0.405 × 0.368 × 0.311 mm^3. Mo Kα (λ = 0.71073 Å), F (000) = 568, T = 293(2) K. The final R values were R_1 = 0.0388, and wR_2 = 0.1093, for 7362 observed reflections [I > 2σ (I)].

Crystallographic data for **8** and **16** have been deposited at the Cambridge Crystallographic Data Centre with the deposition number of CCDC 806237 and 806238, respectively. Copies of the data can be obtained, free of charge, on application to the Director, CCDC, 12 Union Road, Cambridge CB2 1EZ, UK (fax: +44 1223 336033 or data_request@ccdc.cam.ac.uk).

4.3 Cell lines and culture

Human breast cancer MCF-7 and MDA-MB-231 and normal breast MCF-10A cells were obtained from the American Type Culture Collection (Rockville, MD). All cell culture media contained 1% penicillin/streptomycin unless otherwise specified. Human MCF-7 cells were grown in DMEM media containing 10% FBS, 1mM non-essential amino acids, Earle's BSS, 1 mM sodium pyruvate and 10 mg/L bovine insulin. Human MDA-MB-231 cells were grown in DMEM medium containing 10% FBS, 0.1 mM MEM non-essential amino acids, and 2 mM L-glutamine. Human MCF-10A cells were grown in DMEM/F12 media containing 5% horse serum, 100 μg/mL EGF, 1 mg/mL Hydrocortisone, 1 mg/mL cholera toxin, and 10 mg/mL insulin.

4.4 Cell viability assay

The effects of the compounds on human cell growth, presented as the percentage of viable cells, were evaluated by the MTT method [39–40]. Cells were plated on a 96-well plate at $3×10^3$ cells/well and exposed to the test compounds (0, 1, 5, 10, 25, 50 μM) for 72 h. Cultures were also treated with DMSO as the vehicle control. After 72 h of treatment, 10 μL of 3-(4,5-dimethylthiazol-2-yl)-2,5-diphenyltetrazolium bromide (MTT) solution (5 mg/mL; Sigma; St. Louis, MO) was added to each well and the plates were incubated for 2–4 h at 37°C. The supernatant was then removed from formazan crystals and 100 μL of DMSO was added to each well. The absorbance at 570 nm was read using an OPTImax microplate reader. The cell viability was calculated by dividing the mean OD of compound-containing wells by that of DMSO-control wells. Three separate experiments were accomplished to determine the IC_{50} values.

4.5 Cell cycle distribution

For determining effects of the test compound on the cell cycle progression, a previously reported protocol was followed [41–42]. $2–3×10^5$ cells were treated with the test compound (0, 1, 2.5 μM) for 24 h prior to analysis. Cells were trypsinized, washed with PBS, and fixed in 1.5 mL 95% ethanol at 4 °C overnight. The cells were then incubated with RNAse and stained with propidium iodide (Sigma), and the DNA content was further determined by flow cytometry.

4.6 Detection of apoptosis

This assay was carried out as previously described [41–42]. Cells in early and late stages of apoptosis were determined by an annexin V-FITC apoptosis detection kit from BioVision (Mountain View, CA). In brief, $2–3\times10^5$ cells were exposed to the test compound (0, 1, 5 μM) and incubated for 48 h prior to analysis. Media and cells were collected and washed with serum-free media. Cells were then re-suspended in 500 μL of Annexin V binding buffer followed by addition of 5 μL Annexin-V FITC and 5 μL of propidium iodide. The samples were incubated in the dark for 15 min at room temperature and then analyzed with flow cytometry. Cells that were positive for Annaexin V-FITC alone (early apoptosis) and Annexin V-FITC and propidium iodide (late apoptosis) were counted.

Supplementary Material

Refer to Web version on PubMed Central for supplementary material.

Acknowledgments

The work was mainly supported by program NCET Foundation, NSFC(81230090) (to W.-D. Z. and H.-Z. J.), a grant (BCTR070731) from Susan G. Komen for the Cure (to R.Z.), and a Scholarship Award for Excellent Doctoral Student granted by the Chinese Ministry of Education (to J.-J. Q.). W.-D. Z. and H.-Z. J. were also supported by Global Research Network for Medicinal Plants (GRNMP) and King Saud University, Shanghai Leading Academic Discipline Project(B906), FP7-PEOPLE-IRSES-2008 (TCMCANCER Project 230232), Key laboratory of drug research for special environments, PLA, Shanghai Engineering Research Center for the Preparation of Bioactive Natural Products(10DZ2251300) and the Scientific Foundation of Shanghai China (12401900801,09DZ1975700, 09DZ1971500,10DZ1971700), National Major Project of China (2011ZX09307-002-03), and National Key Technology R&D Program of China (2012BAI29B06). R.Z. was also supported by NIH grants R01 CA112029 and R01 CA121211.

References

[1]. Ling, Y. *Inula* L. In: Ling, Y., editor. Flora of China. Science Press; Beijing: 1979. p. 248-281.

[2]. Zhao YM, Zhang ML, Shi QW, Kiyota H. Chemical constituents of plants from the genus *Inula*. Chem. Biodiversity. 2006; 3:371–384.

[3]. Máñez S, del C. Recio M, Gil I, Gomez C, Giner RM, Waterman PG, Rios JL. A glycosyl analog of diacylglycerol and other antiinflammatory constituents from *Inula viscosa*. J. Nat. Prod. 1999; 62:601–604. [PubMed: 10217718]

[4]. Jin HZ, Lee D, Lee JH, Lee K, Hong YS, Choung DH, Kim YH, Lee JJ. New sesquiterpene dimers from *Inula britannica* inhibit NF-κB activation and NO and TNF-α production in LPS-stimulated RAW264.7 cells. Planta Med. 2006; 72:40–45. [PubMed: 16450294]

[5]. Qin JJ, Jin HZ, Zhu JX, Fu JJ, Hu XJ, Liu XH, Zhu Y, Yan SK, Zhang WD. Japonicones E-L, dimeric sesquiterpene lactones from *Inula japonica* Thunb. Planta Med. 2010; 76:278–283. [PubMed: 19742423]

[6]. Nie LY, Qin JJ, Huang Y, Yan L, Liu YB, Pan YX, Jin HZ, Zhang WD. Sesquiterpenoids from *Inula linearifolia* inhibit nitric oxide production. J. Nat. Prod. 2010; 73:1117–1120. [PubMed: 20515062]

[7]. Qin JJ, Jin HZ, Zhu JX, Fu JJ, Zeng Q, Cheng XR, Zhu Y, Shan L, Zhang SD, Pan YX, Zhang WD. New sesquiterpenes from *Inula japonica* Thunb. with their inhibitory activities against LPS-induced NO production in RAW264.7 macrophages. Tetrahedron. 2010; 66:9379–9388.

[8]. Cheng XR, Zeng Q, Ren J, Qin JJ, Zhang SD, Shen YH, Zhu JX, Zhang F, Chang RJ, Zhu Y, Zhang WD, Jin HZ. Sesquiterpene lactones from *Inula falconeri*, a plant endemic to the Himalayas, as potential anti-inflammatory agents. Eur. J. Med. Chem. 2011; 46:5408–5415. [PubMed: 21924800]

[9]. Qin JJ, Zhu JX, Zeng Q, Cheng XR, Zhu Y, Zhang SD, Shan L, Jin HZ, Zhang WD. Pseudoguaianolides and guaianolides from *Inula hupehensis* as potential anti-inflammatory agents. J. Nat. Prod. 2011; 74:1881–1887. [PubMed: 21894898]

[10]. Zhang SD, Qin JJ, Jin HZ, Yin YH, Li HL, Yang XW, Li X, Shan L, Zhang WD. Sesquiterpenoids from *Inula racemosa* Hook. f. inhibit nitric oxide production. Planta Med. 2012; 78:166–171. [PubMed: 22002850]

[11]. Qin JJ, Jin HZ, Fu JJ, Hu XJ, Wang Y, Yan SK, Zhang WD. Japonicones A–D, bioactive dimeric sesquiterpenes from *Inula japonica* Thunb. Bioorg. Med. Chem. Lett. 2009; 19:710–713. [PubMed: 19117757]

[12]. Rafi MM, Bai NS, Ho CT, Rosen RT, White E, Perez D, Dipaola RS. A sesquiterpene lactone from *Inula britannica* induces anti-tumor effects dependent on Bcl-2 phosphorylation. Anticancer Res. 2005; 25:313–318. [PubMed: 15816553]

[13]. Chen CN, Huang HH, Wu CL, Lin CPC, Hsu JTA, Hsieh HP, Chuang SE, Lai GM. Isocostunolide, a sesquiterpene lactone, induces mitochondrial membrane depolarization and caspase-dependent apoptosis in human melanoma cells. Cancer Lett. 2007; 246:237–252. [PubMed: 16697106]

[14]. Tan RX, Tang HQ, Hu J, Shuai B. Lignans and sesquiterpene lactones from *Artemisia sieversiana* and *Inula racemosa*. Phytochemistry. 1998; 49:157–164. [PubMed: 9745767]

[15]. Liu C, Mishra AK, He B, Tan R. Antimicrobial activities of isoalantolactone, a major sesquiterpene lactone of *Inula racemosa*. Chin. Sci. Bull. 2001; 46:498–501.

[16]. Maoz M, Kashman Y, Neeman I. Isolation and identification of a new antifungal sesquiterpene lactone from *Inula viscosa*. Planta Med. 1999; 65:281–282. [PubMed: 17260308]

[17]. Iijima K, Kiyohara H, Tanaka M, Matsumoto T, Cyong JC, Yamada H. Preventive effect of taraxasteryl acetate from *Inula britannica* subsp. *japonica* on experimental hepatitis *in vivo*. Planta Med. 1995; 61:50–53. [PubMed: 7700992]

[18]. Song QH, Kobayashi T, Iijima K, Hong T, Cyong JC. Hepatoprotective effects of *Inula britannica* on hepatic injury in mice. Phytother. Res. 2000; 14:180–186. [PubMed: 10815011]

[19]. Qin JJ, Huang Y, Wang D, Cheng XR, Zeng Q, Zhang SD, Hu ZL, Jin HZ, Zhang WD. Linearіifolianoids A–D, rare unsymmetrical sesquiterpenoid dimers comprised by xanthane and guaiane framework units from *Inula linearіifolia*. RSC Adv. 2012; 2:1307–1309.

[20]. Qin JJ, Wang LY, Zhu JX, Jin HZ, Fu JJ, Li XF, Li HL, Zhang WD. Neojaponicone A, a bioactive sesquiterpene lactone dimer with an unprecedented carbon skeleton from *Inula japonica*. Chem. Commun. 2011; 47:1222–1224.

[21]. Ghantous A, Gali-Muhtasib H, Vuorela H, Saliba NA, Darwiche N. What made sesquiterpene lactones reach cancer clinical trials? Drug Discov. Today. 2010; 15:668–678. [PubMed: 20541036]

[22]. Lu L. Study on effect of *Cordyceps sinensis* and artemisinin in preventing recurrence of lupus nephritis, Chin. J. Integr. Trad. West. Med. 2002; 22:169–171.

[23]. Ito K, Iida T. Seven sesquiterpene lactones from *Inula britannica* var. *chinensis*. Phytochemistry. 1981; 20:271–273.

[24]. Gao F, Wang H, Mabry TJ, Kinghorn AD. Dihydroflavonol sweeteners and other constituents from *Hymenoxys turneri*. Phytochemistry. 1990; 29:2865–2869.

[25]. Yang JL, Wang R, Liu LL, Shi YP. Sesquiterpenoids from *Inula britannica*. Planta Med. 2011; 77:362–367. [PubMed: 20862636]

[26]. Zhang T, Xiao W, Gong T, Yang Y, Chen RY, Yu DQ. Two new eudesmanolides from *Inula racemosa*. J. Asian Nat. Prod. Res. 2010; 12:788–792. [PubMed: 20839127]

[27]. Hoeneisena M, Sicvaa M, Bohlmannb F. Sesquiterpene lactones of *Podanthus mitiqui*. Phytochemistry. 1980; 19:2765–2766.

[28]. Bohlmann F, Zdero C, Ahmed M. New sesquiterpene lactones, geranyllinalol derivatives and other constituents from *Geigeria* species. Phytochemistry. 1982; 21:1679–1691.

[29]. Ohno S, Tomita-Yokotani K, Kosemura S, Node M, Suzuki T, Amano M, Yasui K, Goto T, Yamamura S, Hasegawa K. A species-selective allelopathic substance from germinating sunflower (*Helianthus annuus* L.) seeds. Phytochemistry. 2001; 56:577–581. [PubMed: 11281135]

[30]. Zhang S, Won YK, Ong CN, Shen HM. Anti-cancer potential of sesquiterpene lactones: bioactivity and molecular mechanisms. Curr. Med. Chem. Anticancer Agents. 2005; 5:239–249. [PubMed: 15992352]

[31]. Higuchi Y, Shimoma F, Ando M. Synthetic method and biological activities of cis-fused α-methylene γ-lactones. J. Nat. Prod. 2003; 66:810–817. [PubMed: 12828467]

[32]. Merfort I. Perspectives on sesquiterpene lactones in inflammation and cancer. Curr. Drug Targets. 2011; 12:1560–1573. [PubMed: 21561425]

[33]. Lee KH, Hall IH, Mar EC, Starnes CO, ElGebaly SA, Waddell TG, Hadgraft RI, Ruffner CG, Weidner I. Sesquiterpene antitumor agents: inhibitors of cellular metabolism. Science. 1977; 196:533–536. [PubMed: 191909]

[34]. Shiraki T, Kamiya N, Shiki S, Kodama TS, Kakizuka A, Jingami H. Alpha,beta-unsaturated ketone is a core moiety of natural ligands for covalent binding to peroxisome proliferator-activated receptor gamma. J. Biol. Chem. 2005; 280:14145–14153. [PubMed: 15695504]

[35]. Stewart ZA, Westfall MD, Pietenpol JA. Cell-cycle dysregulation and anticancer therapy. Trends Pharmacol. Sci. 2003; 24:139–145. [PubMed: 12628359]

[36]. Amanatullah DF, Reutens AT, Zafonte BT, Fu M, Mani S, Pestell RG. Cell-cycle dysregulation and the molecular mechanisms of prostate cancer. Front. Biosci. 2000; 5:D372–D390. [PubMed: 10762592]

[37]. Ghobrial IM, Witzig TE, Adjei AA. Targeting apoptosis pathways in cancer therapy. CA Cancer J. Clin. 2005; 55:178–194. [PubMed: 15890640]

[38]. Kasibhatla S, Tseng B. Why target apoptosis in cancer treatment? Mol. Cancer Ther. 2003; 2:573–580. [PubMed: 12813137]

[39]. Li M, Zhang Z, Hill DL, Chen X, Wang H, Zhang R. Genistein, a dietary isoflavone, down-regulates the MDM2 oncogene at both transcriptional and posttranslational levels. Cancer Res. 2005; 65:8200–8208. [PubMed: 16166295]

[40]. Wang W, Zhang X, Qin JJ, Voruganti S, Nag SA, Wang MH, Wang H, Zhang R. Natural product ginsenoside 25-OCH3-PPD inhibits breast cancer growth and metastasis through down-regulating MDM2. PLoS One. 2012; 7:e41586. [PubMed: 22911819]

[41]. Wang W, Rayburn ER, Velu SE, Nadkarni DH, Murugesan S, Zhang R. In vitro and in vivo anticancer activity of novel synthetic makaluvamine analogues. Clin. Cancer Res. 2009; 15:3511–3518. [PubMed: 19451594]

[42]. Yang X, Wang W, Qin JJ, Wang MH, Sharma H, Buolamwini JK, Wang H, Zhang R. JKA97, a novel benzylidene analog of harmine, exerts anti-cancer effects by inducing G1 arrest, apoptosis, and p53-independent up-regulation of p21. PLoS One. 2012; 7:e34303. [PubMed: 22558087]

Highlights

1.) New sesquiterpenoids and their dimers were identified from *Inula linearii folia*;

2.) These sesquiterpenoids exhibited a selective cytotoxicity for tumor cells;

3.) Linearii folianoid E showed the strongest cytotoxicity against tumor cells;

4.) Induction of cell cycle arrest and apoptosis would be key mechanisms of action.

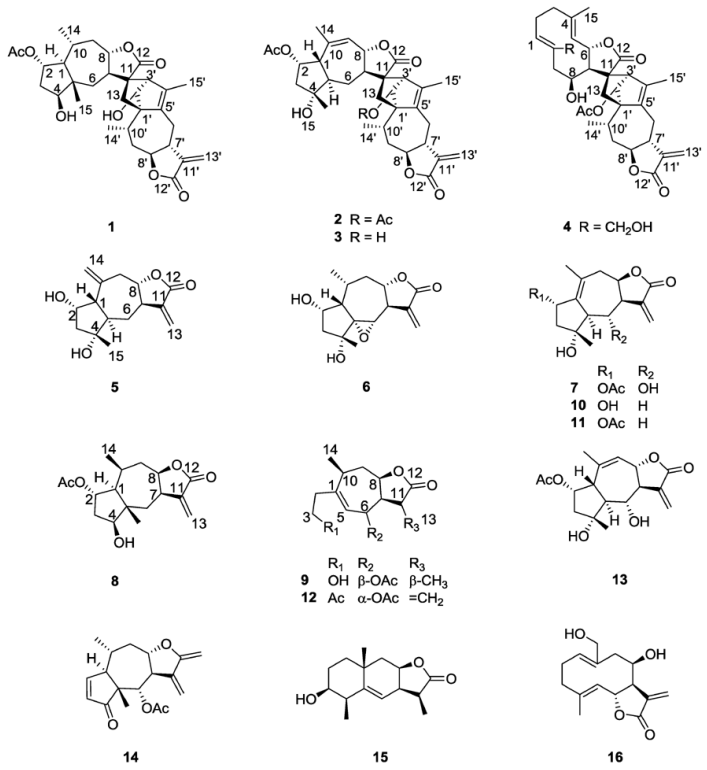

Figure 1.
Structures of compounds **1**–**16**.

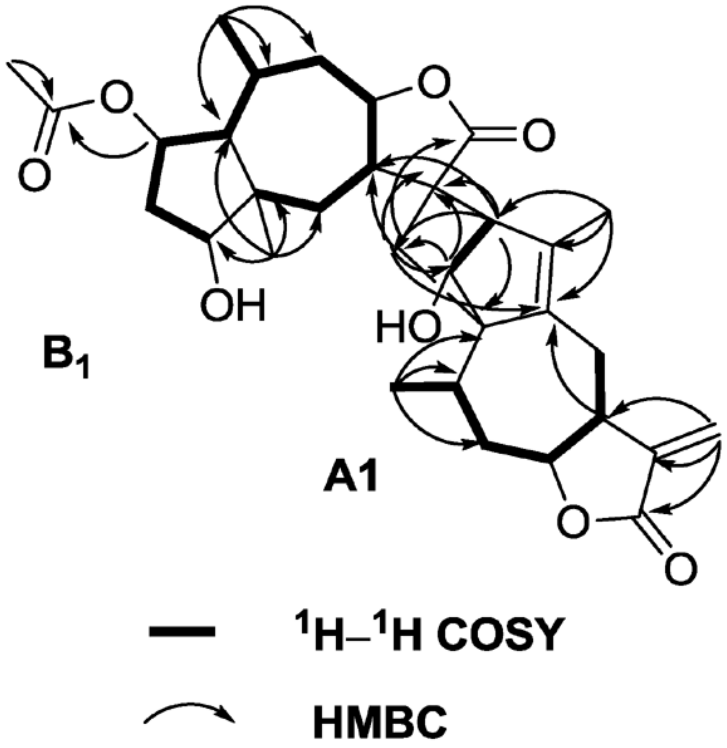

Figure 2.
Key ^{1}H-^{1}H COSY and HMBC correlations of compound **1**.

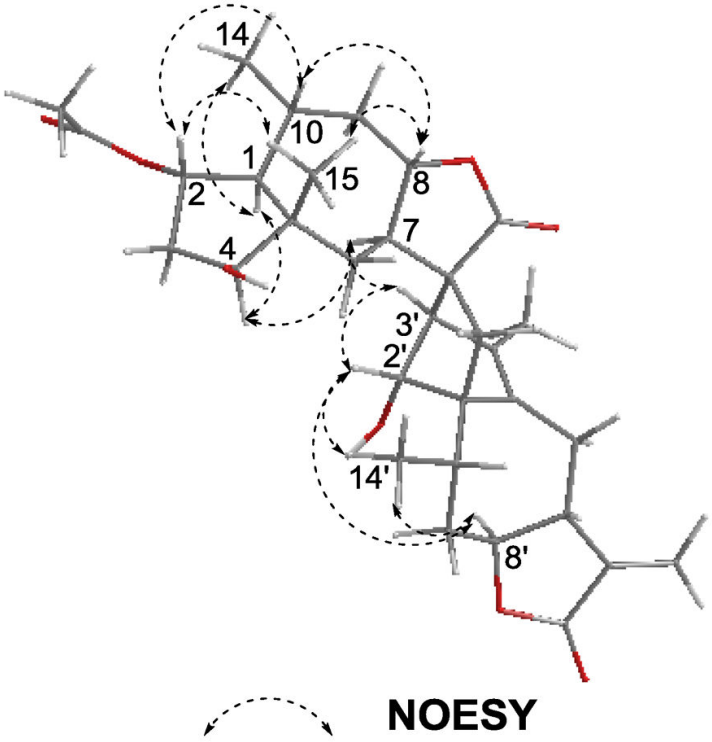

Figure 3.
Key NOESY correlations of compound **1**.

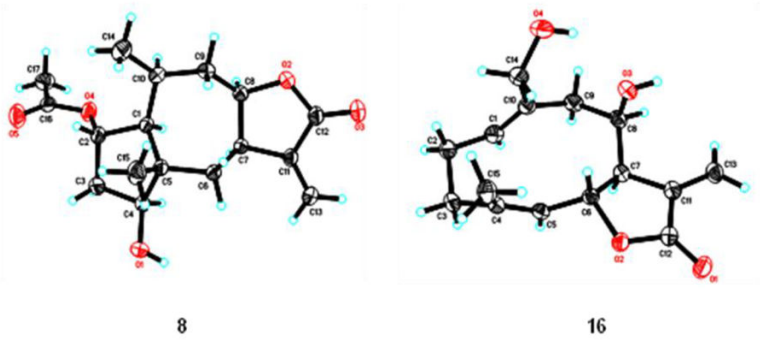

Figure 4.
X-ray crystallographic structures of compounds **8** and **16**.

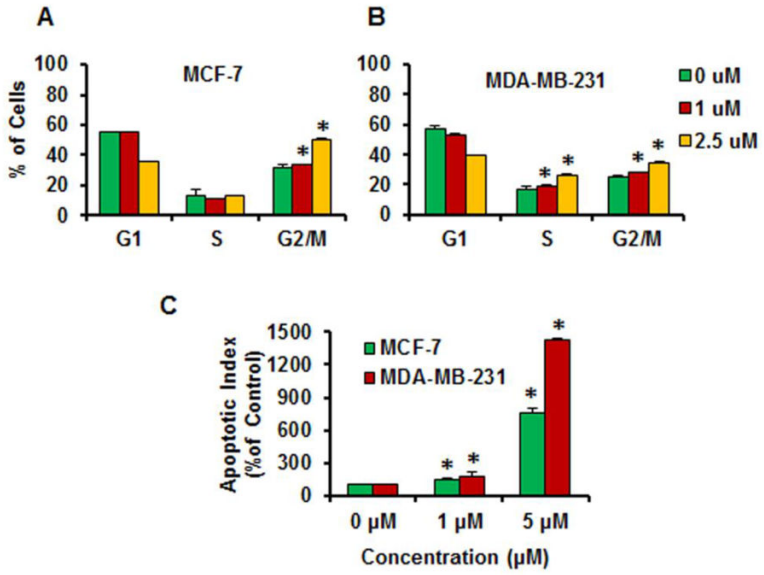

Figure 5.

Effects of lineariifolianoid E (**1**) on the cell cycle progression of human breast cancer MCF-7 (A) and MDA-MB-231 cells (B) in culture. (C) Induction of apoptosis in human breast cancer cells by lineariifolianoid E (**1**). The apoptotic index is in comparison to untreated cells. The values are presented as means ± S.D. and were analyzed by student's t-test. * $P < 0.05$ vs. control group (DMSO).

Table 1

^{1}H (400 MHz) and ^{13}C (100 MHz) NMR data for **1–4** in $CDCl_3$

No.	1		2		3		4	
	δ_C	δ_H (*J* in Hz)	δ_C	δ_H (*J* in Hz)	δ_C	δ_H (*J* in Hz)	δ_C	δ_H (*J* in Hz)
1	53.3 d	1.49 m	51.3 d	2.25 m	51.5 d	2.23 m	135.5 d	5.14 dd (11.4, 4.0)
2	74.1 d	4.83 t (8.0)	75.1 d	5.20 t (3.9)	75.2 d	5.23 t (3.6)	25.9 t	2.25 m; 2.25 m
3	38.6 t	1.89 m; 1.70 m	48.1 t	1.95 m; 1.88 m	48.0 t	1.92 m; 1.90 m	39.6 t	2.35 m; 2.15 m
4	80.6 d	3.49 t (8.7)	78.7 s		78.8 s		143.3 s	
5	44.9 s		51.9 d	1.72 m	52.0 d	1.70 m	128.0 d	4.86 d (9.3)
6	37.0 t	1.41 dd (14.8, 5.1); 1.10 m	28.1 t	1.88 m; 1.17 m	28.5 t	1.85 m; 1.12 m	72.9 d	5.08 dd (9.3, 7.3)
7	48.4 d	2.85 m	50.9 d	2.40 t (10.0)	50.0 d	2.47 t (10.5)	51.5 d	2.65 m
8	83.0 d	4.28 m	80.1 d	4.43 dd (10.0, 2.0)	83.7 d	4.56 dd (10.5, 2.0)	68.9 d	4.63 d (2.9)
9	44.8 t	2.39 m; 1.27 m	128.0 d	5.79 d (2.0)	127.1 d	5.83 d (2.0)	45.8 t	2.83 m; 2.42 dd (14.1, 1.7)
10	28.6 d	1.89 m	135.3 s		136.2 s		134.3 s	
11	58.1 s		55.9 s		57.9 s		55.9 s	
12	184.8 s		176.5 s		184.7 s		182.4 s	
13	33.1 t	2.22 dd (12.6, 3.3); 2.04 m	31.1 t	2.18 m; 2.00 m	32.5 t	2.22 m; 2.00 m	34.7 t	2.35 m; 1.72 m
14	19.6 q	0.94 d (6.6)	22.6 q	1.76 s	22.6 q	1.79 s	60.6 t	4.25 d (11.5); 3.87 d (11.5)
15	18.8 q	0.84 s	25.1 q	1.10 s	25.1 q	1.10 s	17.5 q	1.68 d (0.8)
1′	69.5 s		67.8 s		69.3 s		72.3 s	
2′	85.6 d	3.42 d (9.8)	82.4 d	4.54 s	85.5 d	3.45 d (9.1)	83.6 d	4.47 s
3′	52.6 d	2.62 br s	48.1 d	2.69 s	52.2 d	2.62 br s	48.9 d	2.73 m
4′	140.1 s		138.7 s		139.7 s		139.3 s	
5′	133.9 s		134.8 s		134.4 s		132.8 s	
6′	25.5 t	2.85 m; 2.22 dd (12.6, 3.3)	25.7 t	3.03 dd (16.4, 1.8); 2.18 m	25.8 t	2.96 br d (16.6); 2.15 m	26.2 t	3.04 dd (16.2, 2.6); 1.95 m
7′	45.1 d	2.85 m	44.6 d	2.64 m	44.5 d	2.64 m	45.5 d	2.60 m
8′	81.0 d	4.28 m	81.6 d	4.26 ddd (13.4, 12.1, 3.3)	81.5 d	4.27 ddd (13.0, 12.0, 3.4)	81.0 d	4.06 ddd (12.0, 9.0, 2.6)
9′	36.7 t	2.39 m; 2.04 m	35.6 t	2.30 m; 2.00 m	36.3 t	2.35 m; 2.05 m	35.4 t	2.20 m; 1.90 m
10′	26.7 d	2.85 m	25.2 d	3.21 m	26.4 d	2.87 m	26.1 d	2.58 m
11′	139.7 s		139.2 s		139.4 s		140.1 s	
12′	169.4 s		169.9 s		169.8 s		170.2 s	

No.	1		2		3		4	
	δ_C	δ_H (*J* in Hz)	δ_C	δ_H (*J* in Hz)	δ_C	δ_H (*J* in Hz)	δ_C	δ_H (*J* in Hz)
13′	118.9 t	6.25 d (3.1); 5.60 d (2.8)	119.7 t	6.20 d (3.2); 5.55 d (2.9)	119.6 t	6.21 d (3.3); 5.55 d (3.0)	118.4 t	6.11 d (3.3); 5.44 d (3.1)
14′	18.9 q	1.21 d (7.1)	18.7 q	1.07 d (7.2)	18.9 q	1.20 d (7.2)	18.6 q	1.05 d (8.3)
15′	13.7 q	1.76 s	13.7 q	1.81 d (1.5)	13.7 q	1.78 s	13.5 q	1.83 d (1.6)
2-OAc	170.7 s		170.4 s		170.3 s			
	21.1 q	2.01 s	21.5 q	2.04 s	21.5 q	2.04 s		
2′-OH		6.34 d (9.8)				6.18 d (9.3)		
2′-OAc			170.6 s				169.5 s	
			21.2 q	2.09 s			21.3 q	2.06 s

Table 2

^{1}H (400 MHz) and ^{13}C (100 MHz) NMR data for **5–9**.

No.	5 in $CDCl_3$		6 in $CDCl_3$		7 in $CDCl_3$		8 in $CDCl_3$		9 in CD_3OD		16 in $CDCl_3$	
	δ_C	δ_H(*J* in Hz)	δ_C	δ_H(*J* in Hz)	δ_C	δ_H(*J* in Hz)	δ_C	δ_H(*J* in Hz)	δ_C	δ_H(*J* in Hz)	δ_C	δ_H(*J* in Hz)
1	55.7 d	2.32 dd (12.0, 1.4)	57.4 d	1.80 dd (11.8, 3.0)	130.6 s		49.2 d	1.70 m	152.1 s		134.4 d	5.05 dd (11.4, 4.1)
2	73.4 d	4.39 t (3.6)	74.0 d	4.15 m	73.1 d	5.48 t (7.5)	71.7 d	5.17 ddd (12.0, 10.0, 3.9)	41.8 t	2.50 m; 2.18 m	25.9 t	2.25 m; 2.25 m
3	48.3 t	2.05 d (14.5); 1.87 dd (14.5, 4.4)	47.3 t	2.20 dd (13.0, 5.7); 1.92 dd (13.0, 6.7)	46.8 t	2.54 m; 1.76 dd (12.6, 8.0)	37.8 t	2.11 m; 1.95 m	62.2 t	3.60 m; 3.55 m	39.6 t	2.35 m; 2.15 m
4	80.3 s		71.6 s		78.8 s		74.8 d	3.96 br t (8.2)			142.3 s	
5	51.8 d	2.25 ddd (13.0, 11.8, 2.1)	73.9 s		59.1 d	2.84 m	45.1 s		124.5 d	5.78 d (8.0)	126.8 d	4.86 d (10.0)
6	28.8 t	2.45 dt (13.0, 2.6); 1.12 m	56.5 d	3.21 d (5.7)	71.3 d	3.94 t (9.3)	39.4 t	1.90 m; 1.61 brt (14.5)	69.7 d	5.14 d (8.0)	75.2 d	5.12 dd (10.0, 8.7)
7	50.3 d	2.67 m	50.9 d	2.70 m	52.5 d	2.89 m	37.6 d	3.20 m	46.0 d	2.84 br t (7.0)	53.7 d	2.79 m
8	82.2 d	3.93 ddd (11.7, 10.0, 2.0)	78.0 d	4.05 ddd (12.2, 11.2, 2.6)	77.0 d	3.90 m	79.3 d	4.71 ddd (11.7, 7.9, 3.2)	81.3 d	4.77 m	70.3 d	4.48 d (3.3)
9	42.3 t	3.12 dd (14.8, 2.0); 2.68 m	44.2 t	2.44 dt (13.2, 2.6); 1.55 m	40.9 t	2.67 dd (15.6, 3.0); 2.56 m	35.5 t	2.20 m; 1.80 m	39.61	2.34 m; 2.16m	44.3 t	2.90 dd (14.3, 5.0); 2.41 dd (14.3, 2.0)
10	142.9 s		33.8 d	1.73 m	132.6 s		27.4 d	2.11 m	32.9 d	2.40 m	135.1 s	
11	139.6 s		137.8 s		137.0 s		139.5 s		39.5 d	3.00 m	138.3 s	
12	169.9 s		168.9 s		170.2 s		169.6 s		181.4 s		170.4 s	
13	119.1 t	6.18 d (3.3); 5.53 d (3.1)	121.91	6.35 d (3.5); 5.88 d (3.3)	125.4 t	6.40 d (1.6); 6.31 d (3.0)	123.0 t	6.28 d (2.3); 5.62 d (2.0)	9.6 q	1.06 d (7.0)	120.7 t	6.36 d (3.6); 5.61 d (3.1)
14	115.4 t	5.28 br s; 5.20 d (0.7)	20.3 q	1.16 d (6.3)	23.4 q	1.73 s	16.6 q	1.07 d (7.1)	22.5 q	1.18 d (7.0)	60.5 t	4.14 d (12.0) 3.84 d (12.0)
15	24.6 q	1.25 s	25.1 q	1.24 s	23.8 q	1.28 s	17.8 q	0.97 s			17.2 q	1.68 d (0.9)
2-OAc					170.6 s		170.8 s					
					20.8 q	2.06 s	21.0 q	2.04 s				
6-OAc									171.8 s			
									21.2 q	1.95 s		

Table 3

Effects of compounds **1–16** on viability of human breast cancer cells (MCF-7 and MDA-MB-231) and normal breast cells (MCF-10A).

Compound	IC_{50} (μM)		
	MCF-7	**MDA-MB-231**	**MCF-10A**
1	1.6±0.1	2.8±0.2	27.9±2.3
2	3.4±0.2	10.7±0.7	>50
3	7.8±0.5	16.5±1.3	>50
4	3.7±0.2	5.7±0.5	26.4±2.5
5	13.7±0.6	21.1±1.7	>50
6	>50	>50	>50
7	>50	>50	>50
8	6.7±0.5	12.9±0.9	>50
9	>50	>50	>50
10	>50	>50	>50
11	15.5±0.9	25.8±2.1	>50
12	12.6±1.1	28.6±1.9	>50
13	6.2±0.3	11.4±0.5	>50
14	2.1±0.3	2.3±0.1	26.0±1.2
15	>50	>50	>50
16	6.9±0.4	13.8±1.2	45.7±2.5
Doxorubicin[a] (μM)	0.7±0.06	0.9±0.1	2.8±0.2
Paclitaxel[b] (nM)	75.2±5.8	87.0±9.6	427.0±55.4

[a,b]Positive controls: Doxorubicin (98.0–102.0%, HPLC, Sigma); Paclitaxel (>97.0%, Sigma).